

Observation of magnetic spin correlations in the $\text{LuFe}_{10}\text{Mo}_2$ alloy

This article has been downloaded from IOPscience. Please scroll down to see the full text article.

1995 J. Phys.: Condens. Matter 7 3937

(<http://iopscience.iop.org/0953-8984/7/20/013>)

View [the table of contents for this issue](#), or go to the [journal homepage](#) for more

Download details:

IP Address: 171.66.16.151

The article was downloaded on 12/05/2010 at 21:19

Please note that [terms and conditions apply](#).

Observation of magnetic spin correlations in the $\text{LuFe}_{10}\text{Mo}_2$ alloy

C Christides†, R W Erwin‡ and D Niarchos†

† Institute of Materials Science, National Centre for Scientific Research (NCSR) ‘Demokritos’, 153 10 Agia Paraskevi Attiki, Greece

‡ Materials Science and Engineering Laboratory, National Institute of Standards and Technology (NIST)—Gaithersburg, MD 20899, USA

Received 4 October 1994, in final form 1 February 1995

Abstract. Results of magnetic, medium-resolution neutron diffraction and small-angle neutron scattering (SANS) measurements on a polycrystalline $\text{LuFe}_{10}\text{Mo}_2$ intermetallic alloy show that ferromagnetic (FM) interactions exist between 5 and 325 K, but finite magnetic spin correlations emerge in the examined temperature range. It is observed that in zero applied magnetic field there is no well defined critical point T_c indicating a transition from a paramagnetic to a long-range ordered magnetic phase. A linear variation of magnetization as a function of $T^{3/2}$ remarkably persists up to a temperature that is a large fraction of the T_c for the $\text{LuFe}_{12-x}\text{Mo}_x$ alloys.

1. Introduction

Recently, a series of intermetallic compounds with the formula $\text{RFe}_{10}\text{Mo}_2$ (R = rare earth or Y) has been reported [1, 2] to present magnetic properties similar to systems with finite magnetic correlations. These alloys are members of a class of existing intermetallic compounds with general formula [3] $\text{RFe}_{12-x}\text{TM}_x$ ($2.5 \geq x \geq 1$, for TM = Ti, V, Cr, Si, W, Mo) that crystallize in the tetragonal (space group $I4/mmm$) ThMn_{12} (1:12) type of structure. In this structure there are three inequivalent crystallographic sites for the Fe–TM sublattice (8i, 8j, 8f) and only one site (2a) for the R^{3+} ion. The alloys RFe_{12} cannot exist but the substitution of Fe with other transition elements, which selectively occupy a fraction of the 8i sites only (creating short-range disorder), decreases the enthalpy of the system to form the ThMn_{12} type of structure. The iron sublattice presents uniaxial magnetocrystalline anisotropy and the exchange interactions result in ferromagnetic coupling with relatively high Curie temperatures and magnetization that brings the members with R = Sm into the range of applications for permanent magnets [3]. However, the series of alloys with TM = Mo and $x \approx 2$ are exceptional in their intrinsic magnetic properties in several respects [1, 2]. The observed spin glass-(SG)-like effects in the $\text{LuFe}_{10}\text{Mo}_2$ alloy, which is the subject of the present study, have been attributed to (i) a drastic change in the electronic density of states (DOS) around the Fermi level, caused by the incorporation of extra Mo 4d orbitals [4], which induce an itinerant character in the band ferromagnetism of the Fe–Mo sublattice for the given Mo concentration and (ii) a statistical distribution of Fe–Fe and Fe–Mo interatomic distances that may result in a Gaussian distribution of Fe–Fe exchange interactions, with a relatively reduced positive average value J_0 and a broad width Δ appropriate to create magnetic frustration [1]. By now the SG-like behaviour of $\text{LuFe}_{10}\text{Mo}_2$ has been investigated with common magnetic measurements and ^{57}Fe Mössbauer spectroscopy, which provide

magnetic information on a macroscopic and microscopic scale respectively [1]. Since many experimental and theoretical works have suggested that the magnetization process of re-entrant spin glasses (RSGs) closely connects with the magnetic cluster formation or the domain structure on a medium-range scale (10^2 – 10^4 Å), a small-angle neutron scattering (SANS) experiment (typical resolution of 10 – 10^3 Å) can elucidate this point.

In the present work neutron diffraction and SANS measurements of a powdered, polycrystalline $\text{LuFe}_{10}\text{Mo}_2$ sample have been carried out at temperatures below and above the RSG transition temperature (≈ 210 K) in zero applied magnetic field. The existence of an FM configuration has been identified from the appearance of extra magnetic intensity observed exclusively in the nuclear Bragg reflections of the diffraction pattern. Magnetic measurements provide clear evidence that a $T^{3/2}$ variation of magnetization persists up to a temperature that is a large fraction of the T_c . This spin wave behaviour is similar to that observed in the $\text{Fe}_{1-x}\text{Cr}_x$ crystalline alloys [5], which present RSG properties. The obtained magnetic properties will be discussed in view of similar experimental results of solid solution alloys with RSG transitions.

2. Preliminary details

In setting up a framework for the discussion of dynamical problems we need to discuss the time or frequency dependence of the critical fluctuations. For a Heisenberg ferromagnet at small Q below T_c , the excitation spectrum is comprised of magnons and the characteristic frequency will be the magnon frequency:

$$\hbar\omega_c(Q, T) = D(T)Q^2 \quad (2.1)$$

where $D(T)$ is the spin wave stiffness constant. In the limit of quadratic dispersion law for spin waves (2.1), the expression for the magnetization as a function of field H and temperature T is [5]

$$M_{T,H} = M_{0,0} - (g\mu_B/\rho)(\kappa_B T/4\pi D(T))^{3/2} F(\frac{3}{2}, s) \quad (2.2)$$

where g is the Landé splitting factor, ρ is the density and $F(\frac{3}{2}, s)$ is the Bose–Einstein integral function with $s = \kappa_B T/g\mu_B H$. For $H = 0$, $F(\frac{3}{2}, s)$ becomes the zeta function with $\zeta(\frac{3}{2}) = 2.612$. It was shown [5] that for pure iron a good approximation for $D(T)$ is

$$D(T) = D_0 - D_1 T^2. \quad (2.3)$$

Inelastic neutron scattering (INS) experiments [6, 7] can be used to determine the temperature dependence of D in pure FM and RSG systems. Near the T_c , because of thermal fluctuations, the system breaks up into correlated regions and the magnetization decreases from its saturation value. The resulting decrease in the molecular field reduces the restoring forces for spin waves and critical slowing down occurs. Therefore, D increases from zero at T_c and saturates to a constant value proportional to the average magnetic moment for all $T < T_c$ in a pure ferromagnet [7]. As the spin glass (SG) regime is approached at lower temperatures the long-range order (LRO) is decreased and the assumed reduction of the molecular field might cause the observed decrease in the stiffness constant [7].

3. Experimental details

3.1. Sample preparation and characterization

Samples with nominal composition $\text{LuFe}_{10}\text{Mo}_2$ and mass 10 g each were prepared by arc melting of 99.99% pure starting materials in purified argon atmosphere for the neutron scattering experiment. The as-cast ingots with $x = 2$ were vacuum annealed at 850°C for 5 d and quenched in water. In addition, smaller samples of $\text{LuFe}_{12-x}\text{Mo}_x$ with x in the range 2.3–0.5 were formed in order to investigate the dependence of the FM to RSG transition as a function of the Mo concentration. These samples were heat treated at 1100°C for 2 d in order to minimize the secondary phase of $\alpha\text{-Fe}$. The x-ray diffraction (XRD) patterns, collected with a Siemens D500 diffractometer using $\text{Cu K}\alpha$ radiation, has shown $\alpha\text{-Fe}$ in addition to the 1:12 phase for all the prepared samples. The percentage of $\alpha\text{-Fe}$ has been determined by Rietveld profile analysis to be less than 9% and different for each sample. A minimum $\alpha\text{-Fe}$ content of 5% has been found in the sample that was selected for the neutron scattering experiment. The observation of $\alpha\text{-Fe}$ in large batches of 1:12 polycrystalline ingots can be explained by 'coring' of the high-temperature melted iron phase during the peritectic reaction for formation of the intermetallic compound. The linear variation of the lattice parameters as a function of concentration x and energy dispersive analysis of x-rays (EDAX), which was performed for each alloy in a Philips SEM 515 microscope, indicate that the nominal compositions are approximately correct. EDAX analysis of different surface areas in the same ingot for every sample shows that they are homogeneous within the SEM resolution. Typical magnetic measurements, performed with a Quantum Design MPMSR2 SQUID magnetometer, and ^{57}Fe Mössbauer spectra, collected between 5 and 320 K, confirmed the previously reported SG-like properties [1] for the samples with $x \leq 2$. Magnetic isotherms were obtained between 5 and 300 K over an applied field range 0–5 T.

3.2. Neutron scattering

The neutron scattering experiments were performed at the National Institute of Standards and Technology (NIST) research reactor. The neutron diffraction data in $\text{LuFe}_{10}\text{Mo}_2$ powder were taken on the BT9 triple-axis spectrometer with an incident neutron beam energy of 14.845 meV and Soller collimators $40'-40'-40'-40'$. The (002) reflection plane of a pyrolytic graphite (PG) monochromator and analyser crystal, with a 2 inch PG filter in the incident beam, was used for a medium-resolution scan with a constant step of 0.01 \AA^{-1} in Q and 2 min counting time per point for a wavelength $\lambda = 2.348 \text{ \AA}$.

The SANS measurements were collected in the 8 m SANS instrument, which is located in the guide hall of the Cold Neutron Research Facility (CNRF). Cadmium apertures in the conventional 'pinhole' collimation were used for moderate-resolution measurements with a selected mean wavelength of 5.6 \AA ($\Delta\lambda/\lambda$ (FWHM) of 0.25). The scattered neutrons were detected by a $64 \times 64 \text{ cm}^2$ position-sensitive counter with $10 \times 10 \text{ mm}^2$ resolution, placed 2 m behind the sample. The samples were wrapped in Al foil and placed in a closed cycle refrigerator. All measurements were taken in zero external magnetic field by warming up the sample from 10 to 325 K. Background measurements were collected for every temperature and subtracted from the sample's data. A useful momentum transfer range of $0.02 \leq Q \leq 0.27 \text{ \AA}^{-1}$ was covered. Since in the present experiment we are probing very-long-wavelength correlations ($\lambda = 2\pi/Q \approx 50\text{--}300 \text{ \AA}$), the effects of short-range clusters are probably not important.

4. Experimental results

4.1. X-ray diffraction (XRD)

In order to examine the preferred orientation of the Fe sublattice magnetization as a function of x , we made oriented samples on XRD holders by imposing a magnetic field of 1.7 T with a direction parallel to the sample's and to the x-rays' reflection plane simultaneously. The diffraction profiles of the oriented samples are shown in figures 1 and 2 for two samples with $x = 1.0$ ($T_c > RT$) and $x = 2.0$ ($T_c < RT$), respectively, before and after the orientation. It is obvious that for the low- T_c sample with $x = 2.0$ there is no preferred orientation of the magnetic moment at RT. The $x = 1.0$ sample shows a significant change for the oriented pattern. Specifically, the intensity from the (002) reflection plane is zero and there is a systematic decrease for all the peak intensities with Miller indices (hkl) where $l \neq 0$. Therefore, a uniaxial orientation of the magnetization (along the c axis) exists at RT.

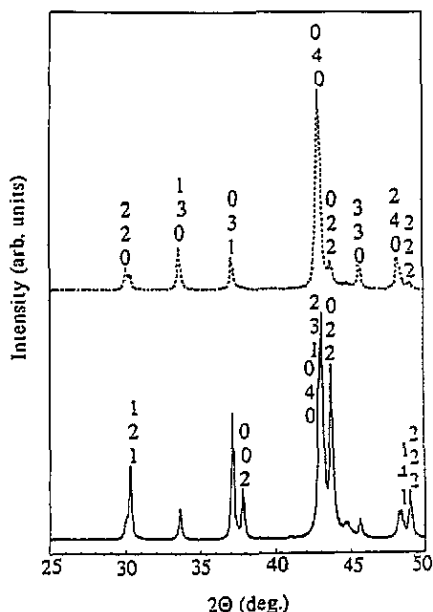


Figure 1. XRD profiles of $\text{LuFe}_{11}\text{Mo}$ for an oriented (dashed line) and a non-oriented (solid line) powder sample.

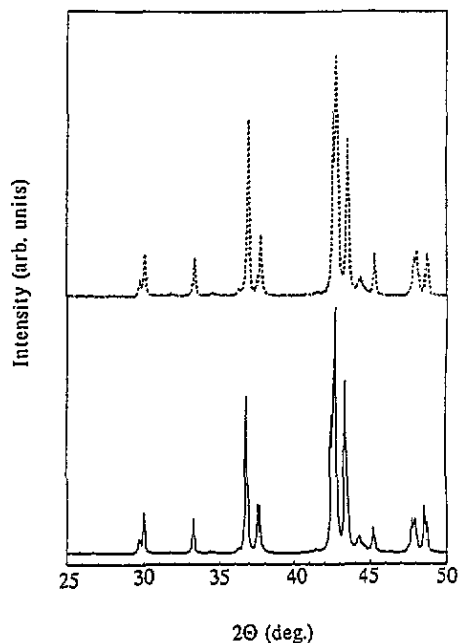


Figure 2. XRD profiles of $\text{LuFe}_{10}\text{Mo}_2$ for an oriented (dashed line) and a non-oriented (solid line) powder sample.

4.2. Magnetic measurements

Transition temperatures T_c from the paramagnetic (PM) to the FM state were determined from thermomagnetic scans in an applied field of 0.005 T (figure 3). The observed T_c values for concentration ranges of $x \leq 1.8$ and $x \geq 2.0$ seem to vary approximately linearly with two different slopes. The anomalous decrease of T_c is evidence that a significant weakening of the Fe exchange interactions occurs as the Mo concentration range $1.8 < x < 2.0$ is approached. Isotherm magnetization curves in the temperature range 5–300 K were obtained. The measurements were collected after zero-field cooling of the samples down

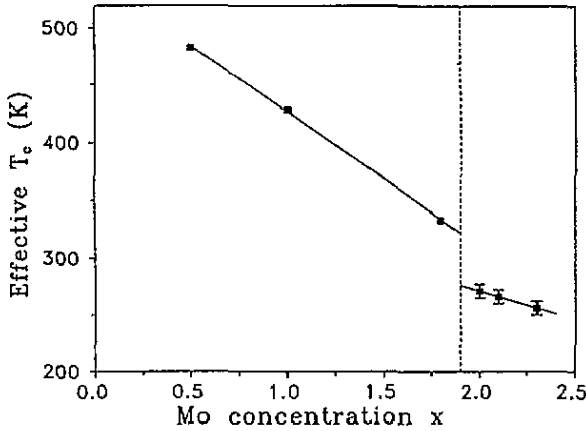


Figure 3. Transition temperatures T_c observed in an applied field of 0.005 T for several Mo concentrations x .

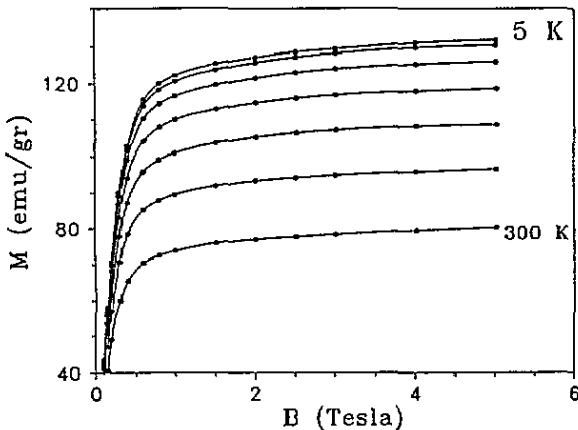


Figure 4. Observed magnetic isotherms of $\text{LuFe}_{11}\text{Mo}$ collected every 60 K.

to 5 K and then by warming up to 300 K. The isotherms for every temperature were taken by decreasing the magnetic field from 5 to 0 T. The experimental magnetic isotherms were corrected for the α -Fe contribution by subtracting the product of the α -Fe percentage, determined from Rietveld analysis, and an $M_s(\text{Fe})$ of 218 emu g^{-1} . The obtained isotherms for Mo concentrations $x = 1.0$ (FM only) and $x = 2$ (RSG behaviour) are shown in figures 4 and 5 respectively. A significant depression (53%) of M_s at 5 K occurs for the sample with $x = 2.0$ relative to that of $x = 1.0$. In addition, the M_s at 300 K for $x = 1.0$ is higher by 10% than the value observed at 5 K for $x = 2.0$. Note that the 30 emu g^{-1} observed at 300 K ($> T_c = 260 \text{ K}$) for $x = 2.0$ are comparatively well below the 55 emu g^{-1} of the Ni metal ($T_c(\text{Ni}) = 630 \text{ K}$) at this temperature.

A plot of $M_{T,H}/M_{0,0}$ against $T^{3/2}$ shows that (2.2) for the quadratic spin-wave dispersion law is obeyed in the range 5–210 K (figures 6 and 7). To obtain an estimation of the temperature-independent part D_0 in (2.3) we have used for the Landé splitting factor the value $g = 2.07$, by making the assumption that the value used in $\text{Fe}_{30}\text{Cr}_{70}$ RSG alloy [5]

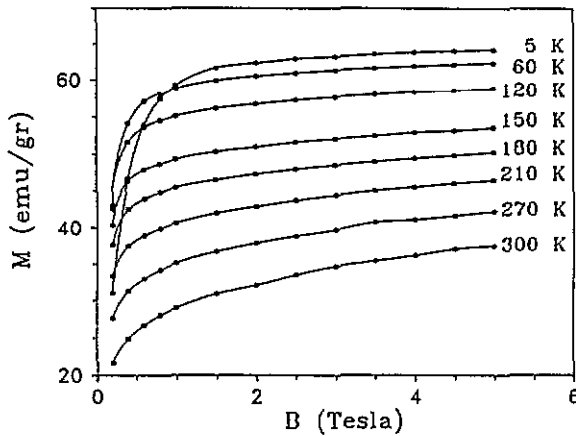


Figure 5. Observed magnetic isotherms of $\text{LuFe}_{10}\text{Mo}_2$.

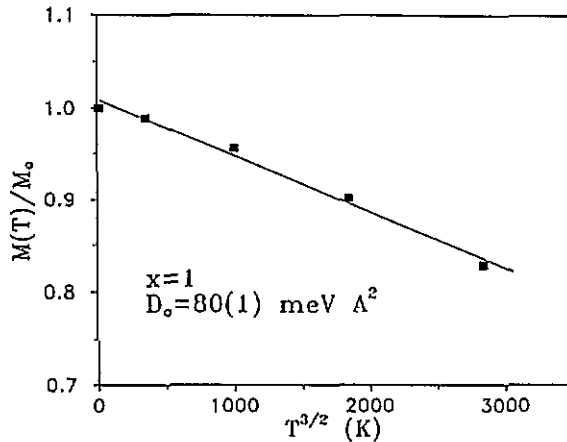


Figure 6. Reduced magnetization data from figure 4, observed at 2 T, plotted as a function of $T^{3/2}$. The solid line is a fit for the slope determination that is used in (2.2) to estimate the spin wave stiffness D . M_0 is the value observed at 5 K.

(with M_s comparable to that observed for $x = 2.0$) must be similar. For the density ρ an estimated value of $8.92(1) \text{ g cm}^{-3}$, obtained from the XRD-determined lattice parameters, has been used. Since D_1 in (2.3) has been found to be a small [5] correction of 3% to D at $T > 150 \text{ K}$, then the estimated D_0 is considered to account satisfactorily for the spin wave stiffness. A linear fitting of the data in figures 6 and 7 gives a slope of $6.17 \times 10^{-5} \text{ K}^{-3/2}$ and $7.89 \times 10^{-5} \text{ K}^{-3/2}$, which correspond to a calculated D_0 of $80(1)$ and $68(1) \text{ meV \AA}^{-2}$, for $x = 1.0$ and 2.0 respectively. This corresponds to 15% softening of the spin wave stiffness as we go from $x = 1.0$ to 2.0 . Since a decrease of magnetization by 20% for $x = 1.0$ and 35% for $x = 2.0$ occurs in the range 5–210 K (figures 4 and 5), the 15% softening in D_0 matches exactly with the relative reduction of the molecular field (expressed indirectly by the magnetization) between the two alloys. Clearly this is a consistency argument showing that the data can be reconciled with this model.

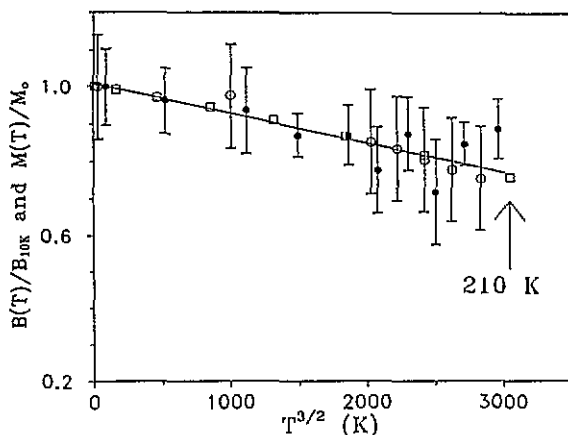


Figure 7. The same plot as in figure 6 for $\text{LuFe}_{10}\text{Mo}_2$. Data from magnetic isothermal measurements (squares) and neutron magnetic Bragg intensity (black circles) follow the same linear variation.

4.3. Neutron diffraction

Two diffraction patterns were collected in the Q range $0.1\text{--}4 \text{ \AA}^{-1}$ at 15 and 300 K (figure 8). The α -Fe peak is relatively stronger in the neutron scattering data because (i) the neutron scattering length b_c of Fe is larger than that of Mo and Lu and (ii) the (330) peak of the 1:12 structure overlaps with the α -Fe peak within our resolution and consequently exaggerates the total Bragg intensity at the position of α -Fe. It is interesting that in the low- Q region (figure 9) a significant small-angle scattering is present above and below the magnetic transition temperature range. At 15 K the low- Q dependence of the diffracted intensity is extended in a broader range of the background.

All the observed Bragg peaks were indexed with the 1:12 structure for both temperatures. The broad peak at $Q = 1.5 \text{ \AA}^{-1}$, which corresponds to (121) and (220) reflection planes, was scanned separately every 20 K in the range 20–325 K. The temperature dependence of the total integrated intensity, extracted from fitting of two Gaussian line-shapes, is presented in figure 10. In order to derive any magnetic intensity I_M in the nuclear Bragg peaks we have subtracted the intensity of the 325 K peak from the observed intensities for all the lower temperatures and then normalized them by dividing by the magnetic integrated intensity of the peak at 20 K. Note that these I_M include an uncertainty from the thermal motion correction (Debye–Waller factor) in the Bragg scattering. Since $I_M \propto M^2$, a plot of $[I_M(T)/I_M(20 \text{ K})]^{1/2}$ against $T/(325 \text{ K})$ should resemble a Brillouin-type function in the case of FM ordering. In figure 10 the observed temperature dependence is plotted together with a Brillouin function of $M(T)$ for spin $\frac{1}{2}$. As seen, the reduced magnetization experimental data points follow the Brillouin curve up to 210 K (0.66 in $T/(325 \text{ K})$). Above that temperature they start to deviate in a way that resembles the behaviour of a pure ferromagnet close to T_c when a high magnetic field is applied.

The coexistence of FM Bragg peaks together with low- Q short-range scattering, in the examined temperature range, is indicative of the formation of short-range ordered FM regions. Further extent of the 15 K low- Q scattering (figure 9) might be associated with these short-range ordered FM regions that start to correlate with one another. To investigate the origin of the low- Q observed scattering SANS measurements were performed.

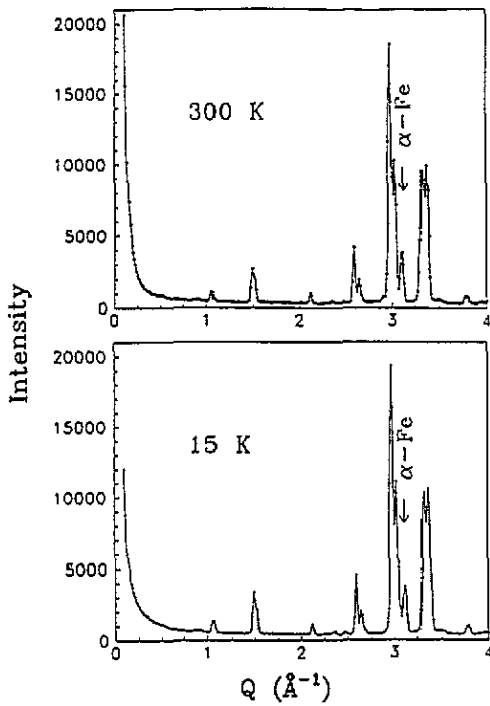


Figure 8. Neutron diffraction patterns of the $\text{LuFe}_{10}\text{Mo}_2$ powder sample used in the SANS experiment. The solid line is a guide to the eye.

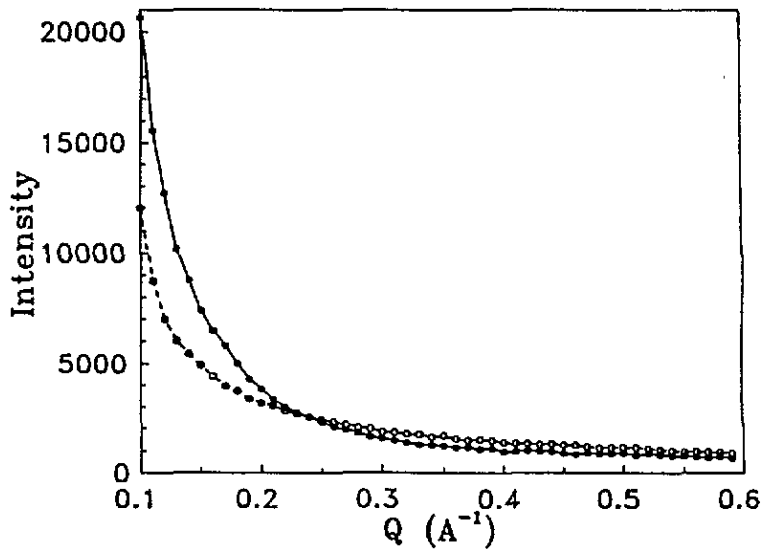


Figure 9. The low- Q range observed in the diffraction pattern of figure 8. The solid line (filled circles) is at 300 K and the dashed line (open circles) is at 15 K.

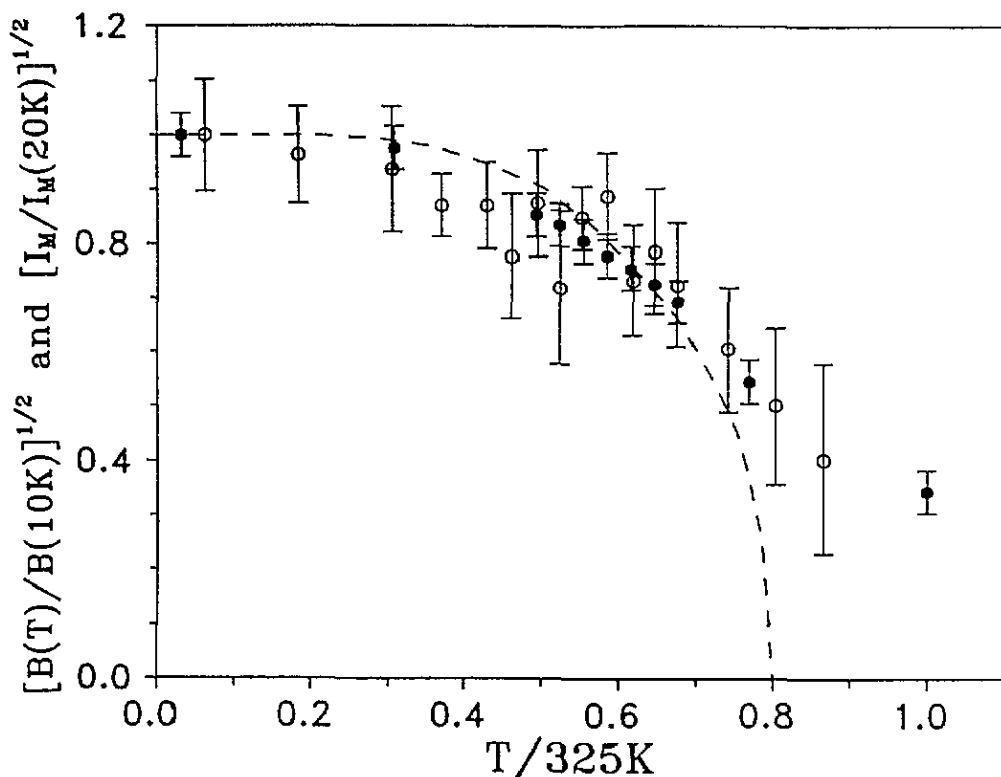


Figure 10. Thermal variation of the obtained magnetic Bragg integrated intensity $I_M(T)$. The dashed line represents a Brillouin function with spin $\frac{1}{2}$ and $T_c = 260$ K. Open circles from neutron and filled circles from magnetization measurements.

4.4. The SANS experiment

SANS measurements were performed for the $\text{LuFe}_{10}\text{Mo}_2$ sample only. The Q dependence of the SANS scattering intensity of RSG materials has been generally expressed by various scattering functions such as the Lorentzian, the squared Lorentzian and the sum of Lorentzian and the squared Lorentzian [8,9]. In a conventional FM system the increase in spatial coherence of the spin fluctuations as T approaches T_c gives rise to a Lorentzian cross-section form, proposed by Ornstein and Zernike [10], within the static approximation. Then

$$I(Q) \propto A/(Q^2 + \kappa^2). \quad (4.1)$$

A plot of the inverse observed intensity versus Q^2 in figure 11 shows clearly that there is a deviation from the Lorentzian form below 250 K. Since the crystal structure is tetragonal (uniaxial), an estimation of the correlation length ξ ($= 1/\kappa$) from the powdered polycrystalline sample cannot be reliable because the observed scattering is the average of the correlations of spin fluctuations along the c axis and the correlations in the a - b lattice plane. It has been observed that a warming up of the sample above 350 K causes a rapid precipitation of α -Fe that decomposes the 1:12 phase. Therefore, practically no real critical point was observed, leading to a pure PM state, up to the imposed phase stability limit of 350 K. Consequently, the current results may provide a qualitative description for the magnetic system in the examined temperature range.

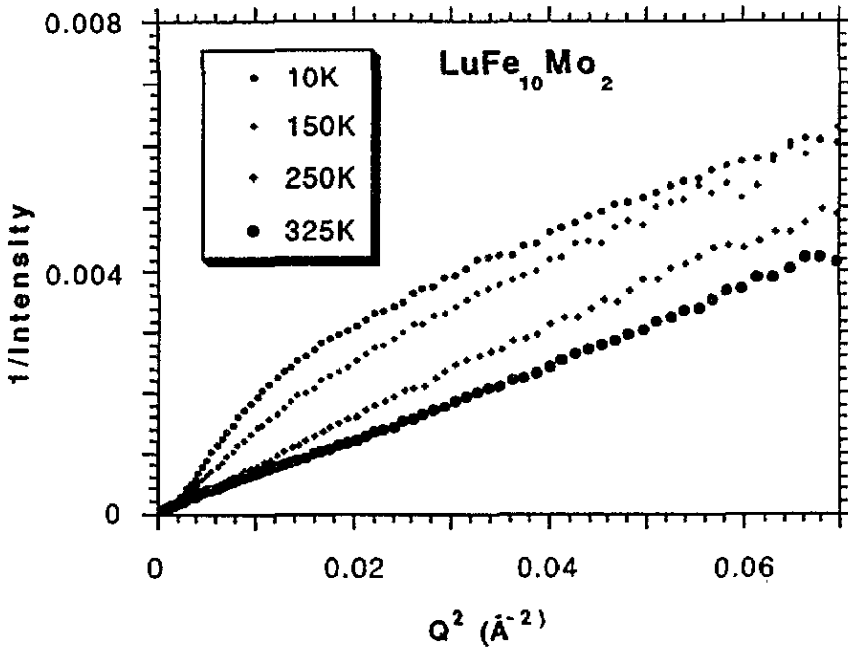


Figure 11. Plots of the inverse intensity against Q^2 , observed in SANS data at four characteristic temperatures.

5. Discussion and conclusions

The present neutron scattering experiment provides for the first time information about the spatial magnetic configurations of $\text{LuFe}_{10}\text{Mo}_2$, which, taken with other measurements, begins to describe the anomalous temperature-dependent behaviour occurring in this alloy [1]. So far, the existing experimental results from magnetic and ^{57}Fe Mössbauer measurements [1] were indicative of the following. (i) An SG-like behaviour appears below 220 K. Close to this temperature, irreversibility sets in in the DC zero-field-cooled (ZFC) and field-cooled (FC) thermomagnetic measurements. At the same temperature the AC susceptibility χ' signal increases and exhibits a peak centred at 180 K. (ii) In a small applied DC magnetic field (≥ 20 Oe) a marginal FM-like T_c of 260 K occurs whereas the AC susceptibility signal remains constant at a non-zero value above 220 K. (iii) Strong relaxation effects occur above 100 K in the zero-field Mössbauer spectra.

The present bulk magnetic and neutron scattering measurements are evidence for the following.

(i) An anomalous dependence upon Mo concentration x of the magnetic ordering transition temperature T_c (figure 3), which can be related to a softening of the exchange interactions, exists. The small Mo concentration (15%) and the local short-range disorder, created in the preferably half-Mo-occupied 8i site, are strong indications that a percolation threshold $p_c > 0$ for an x_c of about two cannot sustain spatially distributed finite clusters, isolated magnetically from each other. Therefore, the observed softening of the exchange interactions for $x > 1.8$ is very likely to be connected with a change in the occupancy and the electronic density of states around the Fermi level that enhance the itinerant character of the band magnetism.

(ii) Non-zero neutron Bragg magnetic scattering persists well above 260 K. In accordance, the previously observed [1] Mössbauer spectrum at 250 K appears to be a strongly relaxed doublet for zero applied magnetic field. Consequently we may conclude that the observed transition at 260 K in a very small DC applied field might be a pseudo- T_c . Thus, it is not clear whether there is a real PM-FM critical phase transition for $T > 220$ K. The temperature dependence of the magnetic Bragg intensity (figure 10) shows that the FM-like critical region is unusually large. Specifically, the decrease of the FM-ordered moment starts at 200 K and extends very smoothly up to 320 K.

(iii) The XRD patterns of the oriented samples (figures 1 and 2) indicate clearly that the magnetic configuration of $\text{LuFe}_{10}\text{Mo}_2$ at RT is not uniaxial.

(iv) The magnetic SANS intensity shows a deviation from the Lorentzian form below 250 K, which can be attributed to scattering from correlation of short-range ordered FM regions below that temperature.

(v) A fit of the reduced order parameter as a function of $T^{3/2}$ follows up to 210 K the behaviour that is expected from a quadratic (FM-order) dispersion law for spin waves. It is clear that dynamic effects affect, as a function of the external thermal and magnetic energy, the intrinsic response of spin correlations in $\text{LuFe}_{10}\text{Mo}_2$. It is remarkable that a $T^{3/2}$ variation of magnetization persists up to a temperature that is a large fraction of the T_c . For the $\text{LuFe}_{11}\text{Mo}$ sample, where a $T_c = 440$ K can be defined, (2.2) holds up to $0.48T_c$, which is a much larger temperature range than the one observed in *crystalline* ferromagnets, where deviations from $T^{3/2}$ behaviour began to dominate beyond $0.15T_c$. This effect is similar to that observed in $\text{Fe}_{1-x}\text{Cr}_x$ alloys [5], where a $T^{3/2}$ variation persists up to $0.49T_c$ for $x \geq 0.5$. The same behaviour has been observed in amorphous FM alloys where a $T^{3/2}$ variation of magnetization exists [11] up to $0.2-0.4T_c$. This effect can be related to the broad distribution of Fe-Fe exchange interactions J_{ij} , centred about a specific positive average value J_0 , which is common in amorphous ferromagnets and crystalline RSG alloys. The reduced ratio value $D_0/T_c = 0.18 \text{ meV } \text{Å}^2 \text{ K}^{-1}$ in $\text{LuFe}_{11}\text{Mo}$, as compared to the value of 0.27 ($= 281 \text{ (meV } \text{Å}^2)/1043 \text{ K}$) for α -Fe, can be considered as a measure for the range of the exchange interactions [12]. The existing ambiguity about the T_c of $\text{LuFe}_{10}\text{Mo}_2$ restricts the application of the previous expressions for a quantitative estimation in this alloy.

In summary, the obtained results support the existence of finite magnetic correlations, which coexist with the FM spin arrangement in the $\text{LuFe}_{12-x}\text{Mo}_x$ alloys for $x > 1.8$. The present data are not adequate to justify the critical behaviour in the range 200–350 K, which has to be investigated in a future experiment with inelastic neutron scattering and magnetic measurements by observing the variation of the order parameter along the inequivalent lattice directions on single crystals.

Acknowledgments

It is a pleasure to acknowledge Dr C Papatriantafillou for helpful discussions on this work. We thank Mr A Petras and V Vlessides for performing XRD and SQUID magnetic measurements. This work has been partially supported from a BRITE/EURAM contract No CT-91-405.

References

- [1] Christides C, Kostikas A, Zouganelis G, Psycharis V, Kou X C and Grossinger R 1993 *Phys. Rev. B* **47** 11 220

- [2] Christides C, Kostikas A, Kou X C, Grossinger R and Niarchos D 1993 *J. Phys.: Condens. Matter* **5** 8611
- [3] Li Hong-Shuo and Coey J M D 1991 *Handbook of Magnetic Materials* vol 6, ed K H J Buschow (Amsterdam: North-Holland) p 1
- [4] Christides C, Li Hong-Shuo, Kostikas A and Niarchos D 1991 *Physica B* **175** 329
- [5] Aldred A T 1976 *Phys. Rev. B* **14** 219
- [6] Motoya K, Shapiro S M and Muraoka Y 1983 *Phys. Rev. B* **28** 6183
- [7] Fincher C R, Shapiro S M, Palumbo A H and Parks R D 1980 *Phys. Rev. Lett.* **45** 474
- [8] Aeppli G, Shapiro S M, Birgeneau R J and Chen H S 1983 *Phys. Rev. B* **28** 5160
- [9] Shapiro S M, Fincher C R, Palumbo A C and Parks R D 1981 *Phys. Rev. B* **24** 6661
- [10] Ornstein L S and Zernike F 1914 *Proc. Sect. Sci. K. Med. Acad., Wet.* **17** 793
Fincher M E 1951 *J. Math. Phys.* **5** 869
- [11] Moorjani K and Coey J M D 1984 *Magnetic Glasses* ed S P Wolsky and A W Czanderna (Amsterdam: Elsevier) pp 133-7
- [12] Keffler F 1966 *Handbuch der Physik* vol 18, ed S Flugge (Berlin: Springer) part 2, p 1